J. Fluid Mech. (1983), *vol.* 129, *pp.* 251–264
Printed in Great Britain

Stability and heat transfer of rotating cryogens. Part 1. Influence of rotation on the onset of convection in liquid ^{4}He

By P. G. J. LUCAS†, J. M. PFOTENHAUER AND R. J. DONNELLY

Department of Physics, University of Oregon, Eugene, OR 97403, U.S.A.

(Received 4 October 1982)

Equipment is described for performing measurements of the Rayleigh–Bénard instability in a sample of rotating liquid ^{4}He. Data are presented on the dependence of the critical Rayleigh number for the onset of convection on Prandtl number in the range $0{\cdot}49 < Pr < 0{\cdot}76$ and over a range of dimensionless angular velocities $0 < \Omega < 200$. Evidence for the existence of subcritical convection is presented.

1. Introduction

Since the pioneering work of Chandrasekhar (1953), there has been a steady interest in rotating Bénard systems which has paralleled that in the more traditional stationary problem. Part of the impetus for this lies in the application to motion in planetary atmospheres, but there are features of intrinsic interest that are unique to rotating systems, for example the Küppers–Lortz (1969) instability. Theoretical work has, in general, been ahead of experimental studies which have been relatively sparse. The technical advantages of using cryogenic fluids for such studies as summarized by Ahlers (1975), combined with the fact that many of their fluid parameters lie outside the range of conventional fluids, provide compelling reasons for using them for experiments. Since the initial experimental work on liquid and gaseous ^{4}He of Ahlers (1974), considerable literature on ^{4}He has appeared (e.g. Walden & Ahlers 1981; Behringer & Ahlers 1982; Maurer & Libchaber 1980), as well as on ^{3}He–^{4}He liquid mixtures both normal (Lee, Lucas & Tyler 1979) and superfluid (Warkentin *et al.* 1980). Nevertheless, apart from our own recent brief report (Lucas, Pfotenhauer & Donnelly 1981), there has been no published work on Bénard convection in rotating cryogenic fluids. Here we present a more detailed account of our measurements of the critical Rayleigh number for the onset of convection in rotating liquid ^{4}He and which we intend to be the first of a series. We have also made detailed heat-transport measurements which will be the subject of a future paper.

2. Background to the present study

The system we have investigated experimentally approximates to the theoretical problem of convection in a rotating homogeneous fluid contained within a cylindrical Rayleigh–Bénard experimental cell with rigid upper and lower boundaries at different temperatures T_C and T_F respectively and finite aspect ratio $\Gamma = D/2d$, where D and d are the diameter and vertical height respectively and where the Boussinesq

† Permanent address: Department of Physics, The University, Manchester M13 9PL, England.

approximation prevails. It is well known that when transformed to a system of coordinates rotating with the fluid, the effect on the equations of fluid motion is to add additional centrifugal and Coriolis terms. However, in theoretical treatments of this problem it is customary to neglect the centrifugal force by assuming it to be small compared with gravity, leaving only the contribution of the Coriolis force.

A recent article by Clever & Busse (1979) summarizes much of the current progress in the theoretical understanding of the problem under these conditions. Linear stability analyses predict that for Prandtl numbers Pr in excess of some critical value Pr_c the onset state is stationary and that the corresponding critical Rayleigh number R_c depends only on angular velocity Ω. These analyses also predict that for $Pr < Pr_c$ an oscillatory convection state with angular frequency σ will have a Rayleigh number Ra_0 at onset which depends on Pr and which can be less than R_c if Ω is sufficiently large. Numerical data on the dependence of $R_c(\Omega)$, $Ra_0(\Omega, Pr)$ and $\sigma(\Omega, Pr)$ on Ω and Pr is provided by this linear theory (Chandrasekhar 1961; Clever & Busse 1979). In the above $\Omega = \Omega_D d^2/\nu$ and $\sigma = \sigma_D d^2/\nu$ are dimensionless angular velocities and frequencies respectively, Ω_D and σ_D are the respective dimensioned quantities and ν is the kinematic viscosity. $Pr = \nu/D_T$, where D_T is the thermal diffusivity, and the Rayleigh number Ra is defined by $Ra = gd^3\beta_p \Delta T/\nu D_T$, where $\Delta T = T_F - T_C$ is the temperature difference across the cell, g is the acceleration due to gravity, and β_p is the thermal-expansion coefficient.

It is worth noting here that the calculations of Clever & Busse (1979) using linear theory predict that if $Pr > 0{\cdot}2$ the onset state is stationary unless $\Omega > 100$. In the experiments to be described in §2 the minimum Prandtl number of liquid ^{4}He attained was 0·49 at a temperature of 2·63 K, so that linear theory predicts that observation of overstability in liquid ^{4}He requires angular velocities Ω well in excess of 100.

Linear theory does not cover adequately the situation when $Pr < 1$ and subcritical finite-amplitude convection can occur and affect the heat transport. The term subcritical is used because this convection can occur even for Rayleigh numbers below Ra_0 or R_c. Calculations of this effect are provided by Veronis (1968) and Clever & Busse (1979). Further finite-aspect-ratio calculations exist by Daniels (1978) and Charlson & Sani (1970).

Diagrams of stability boundaries in (Ra, α)-space for $\Omega < \Omega_c = 27{\cdot}4$ (where α is a dimensionless wavenumber) are provided by Clever & Busse (1979), but if this condition is not satisfied doubt exists about the space and time dependence of the onset state. In fact, Küppers and Lortz (Küppers & Lortz 1969; Küppers 1970) have shown that no two-dimensional parallel-roll solution is stable for $\Omega > 27{\cdot}4$ in the limit of $Pr \to \infty$. Recently Busse (1981) has speculated that a hexagonal cell structure fluctuating in time may be the preferred convection state.

Previous experimental rotation studies were limited to mercury, water and silicone oil with Prandtl numbers of 0·025, 6·8 and of the order of 100 respectively. An early group of studies on water and mercury (Nakagawa & Frenzen 1955; Fultz & Nakagawa 1955; Dropkin & Globe 1959; Goroff 1960) confirm the linear-theory results in general, although the experimental results for Ra_0 are higher than predicted by about a factor of 2. A more detailed study on the same two fluids by Rossby (1969) improves the agreement for mercury provided that $\Omega > 160$, but the data for R_c falls below that predicted by linear theory when $\Omega < 70$. In the same study there is good agreement with linear theory for water if $\Omega < 100$, but experimental values of R_c are lower for higher angular velocities. Koschmieder (1967) had earlier demonstrated the existence of subcritical convection induced by centrifugal forces in oil layers, and

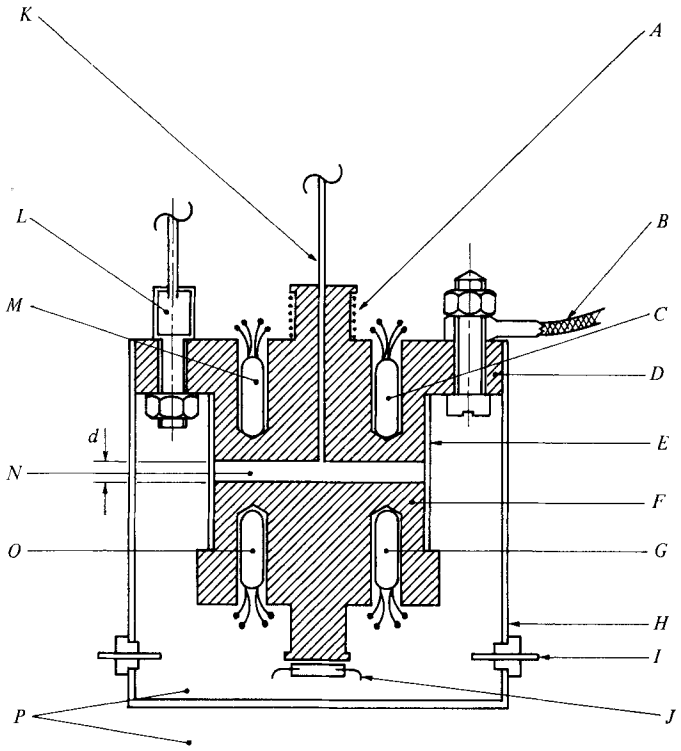

FIGURE 1. Rayleigh–Bénard experimental cell: *A*, heater H_C; *B*, copper-braid heat leak to bath; *C*, germanium resistance thermometer R_{DC}; *D*, copper upper (C) cell boundary maintained at temperature T_C; *E*, 0·025 cm low-conductivity stainless-steel cell wall; *F*, lower (F) cell boundary; *G*, thermometer R_{DF}; *H*, copper thermal shield clamped to upper boundary; *I*, feed-through; *J*, heater H_F; *K*, 0·025 cm stainless-steel filling capillary; *L*, vapour-pressure bulb; *M*, thermometer R_C; *N*, volume occupied by fluid; *O*, thermometer R_F; *P*, vacuum. For clarity, the thermal anchors and leads are not shown.

it is possible that this is at least partially responsible for some of the discrepancies between the experimental studies and linear theory. Krishnamurti's (1971) study on water and silicone oil shows a transition from steady to unsteady flow with increase in angular velocity that provides values of Ω_c of the same order as those predicted by Küppers (1970). A similar transition was also observed by Rossby (1969).

With this background in mind we present our investigations in rotating liquid ^{4}He Bénard convection.

3. Equipment

3.1. *Experimental cell*

The Bénard experimental cell used for the present measurements is suspended inside a stainless-steel vacuum can using a rigid stainless-steel support. The can is surrounded by a pumped superfluid liquid-helium bath maintained at a temperature T_B of about 2·0 K to a stability of $\pm 2{\cdot}5\ \mu$K with the aid of an electronic regulator.

The details of the cell are shown in figure 1. The volume occupied by liquid ^{4}He is cylindrical with diameter $2{\cdot}49 \pm 0{\cdot}005$ cm, height $0{\cdot}1595 \pm 0{\cdot}0007$ cm and axis vertical. The mean temperatures T_C and T_F of the upper 'controlled' and lower 'floating' boundaries are measured with germanium resistance thermometers R_C and R_F. The difference in temperature ΔT between the boundaries is measured with the

pair of thermometers R_{DC} and R_{DF} connected differentially. Each of R_C, R_F and the pair R_{DC} and R_{DF} are part of separate a.c. resistance bridges, each of which is capable of detecting temperature changes of the order of 1 μK. The R_C and R_F bridges are Linear Research LR-110 commercial instruments. The bridge that measures ΔT is an automatically balanced bridge fully described by Lucas & Donnelly (1981).

The temperature difference ΔT is achieved by passing a d.c. current through a metal-film resistor H_F (4·0 kΩ) thermally anchored to the F-boundary. The thin-wall stainless-steel construction of the vertical boundary minimizes that fraction of the heat current produced that reaches the C-boundary through the walls. The magnitude of the heat current is measured by separate pairs of voltage and current leads across H_F. We point out at this stage that, while the gap between the copper C-boundary and the stainless-steel wall is filled with silver solder in the region where the wall passes over the copper, this is not true about the F-boundary. Here thermal contact between the copper and stainless is assumed good owing to a press-fit construction, and when the cell is full, owing to liquid helium filling any gaps.

The heater H_C is thermally anchored to the C-boundary and is used to maintain a temperature difference $T_C - T_B$ across a copper-braid heat leak connected between the C-boundary and the bath, where T_C is above the λ-point of liquid ^{4}He. T_C is regulated to within $\pm 2{\cdot}5$ μK by the action of negative feedback from the R_C bridge null-detector signal to the heater H_C.

The entire lower half of the cell is surrounded by a copper container thermally anchored to the C-boundary. This thermal shield reduces radiation heat leaks into the F-boundary to an extremely low level. It also acts as a convenient platform for locating electrical leads, all of which are attached to feed-throughs around the perimeter of the shield. The thermal shield is not intended to be a vacuum seal.

All resistance thermometer leads are 0·005 cm varnished constantan and are thermally anchored to the boundary whose temperature is being measured as close as is practical to the relevant thermometer. The anchoring is achieved by wrapping the leads several turns round copper posts screwed into the boundaries and painting with G.E. 7031 varnish and subsequently checking for zero electrical contact between the leads and the posts. A 3-lead technique is used in the LR-110 bridges to minimize the effects of lead resistance. Lead compensation is not used in the automatic bridge so that the leads are included in the thermometer calibration. Partial compensation occurs in any case since R_{DC} and R_{DF} are a matched pair. The heater leads are 0·005 cm I.M.I. Niomax superconducting wire to eliminate power dissipation except in the heaters.

From the shield feed-throughs the leads pass up the can and are located again on a tag-board near the top of the can, whence they increase in size to 0·025 cm constantan to reduce their electrical resistance and are thermally anchored to the bath. From this tag-board they pass up inside a stainless-steel vacuum tube and out of the top of the cryostat via vacuum feed-throughs. This arrangement is used rather than passing the leads through the bath to avoid leads resistance changes via bath-level changes. The use of constantan rather than copper further reduces this effect.

The cell is filled via a 0·025 cm diameter stainless-steel capillary tube passing through the C-boundary. This fill line passes out of the can through a separate vacuum tube located within the bath. A second fill line inside another vacuum tube within the bath passes into the can to a copper vapour-pressure bulb anchored to the C-boundary. The second fill line has internal diameter 0·08 cm, which is sufficiently large to render the thermomolecular pressure correction negligible (White 1979). This bulb is necessary to calibrate the thermometers, and we have used both ^{4}He and ^{3}He

gas for this purpose. Care was taken to ensure that neither fill line touched the inside of the vacuum tubes surrounding them. In the case of the cell fill line this avoided the liquid in the fill line becoming superfluid and consequently introducing a temperature-dependent heat leak into the C-boundary. In the case of the vapour-pressure bulb this avoided vapour-pressure measurement errors, the measurement instrument being a Texas Instrument Pressure Gauge Model No. 145.

3.2. *Electronic equipment*

Much of our raw data are in the form of readings of the resistance ratio $S = R_{DC}/(R_{DC}+R_{DF})$ and the power W_F being dissipated in H_F, taken in pairs. All of the electronic equipment used to take this data is under control of a Hewlett-Packard 21 MX minicomputer, most instruments communicating through a common Hewlett-Packard Interface Bus (IEEE-488). The programmable equipment comprises the automatic bridge (Lucas & Donnelly 1981), which measures the ratio $R_{DC}/(R_{DC}+R_{DF})$, a Hewlett-Packard 59501A power supply and Hewlett-Packard 7225A plotter.

The data were stored on disks and recalled later for further processing, but during an experimental run were graphed to provide a monitor of the experiment.

3.3. *Rotating cryostat*

With the exception of the plotter and the computer all of the above electronic equipment and the LR-110 resistance bridges were mounted on the University of Oregon 1 metre rotating table (see figure 2) which is capable of being rotated at any set speed up to 100 rev. min^{-1} using a Graham transmission and belt drive from a fixed-speed motor. The nitrogen-cooled helium Dewar was suspended through a hole in the centre of the platform, and the helium bath was pumped through a 10 cm diameter rotating vacuum seal. All electric leads including the IEEE-488 bus passed through a 25-way commercial slip-ring (type 1067, Fabricast, Inc. So. El Monte, CA) and no difficulty was experienced using the bus despite the lack of shielding and change of line impedance.

4. Preliminary measurements

4.1. *Heat leaks*

As mentioned in §3.1, a thermal shield surrounding the entire cell is expected to reduce radiation heat leaks into the cell. The following measurements (as suggested by Behringer & Ahlers 1982) were taken to establish how well this shield functions. With the cell filled with ^{4}He and zero heat applied to H_F, measurements of the resistance ratio S were taken below and above T_λ. One expects stray heats to produce a temperature difference across the cell above T_λ but not below T_λ (stray heat inputs are thermally shorted through by the superfluid below T_λ). The value S decreases with increased controlled temperature T_C but increases with a temperature difference ΔT across the cell. Thus any stray heat inputs causing a ΔT would be very noticeable as one stepped T_C from below T_λ to above T_λ. Figure 3 shows the results of this test. To gain an upper bound on the possible stray heat into the cell, the stepping procedure described above was accomplished with 0, 0·25 and 1·00 μW heats applied to H_F. Comparing the scatter in S_0 (values of S with zero heat) to the displacement $S-S_0$ with 0·25 μW and 1·00 μW applied gives an upper bound of order 10^{-8} W for stray heat into the cell. This upper bound is of the order of the self-heating of the thermometers in the cell, and two orders of magnitude smaller than the heat inputs required for convection. The slope dS/dT with zero power applied remained the same

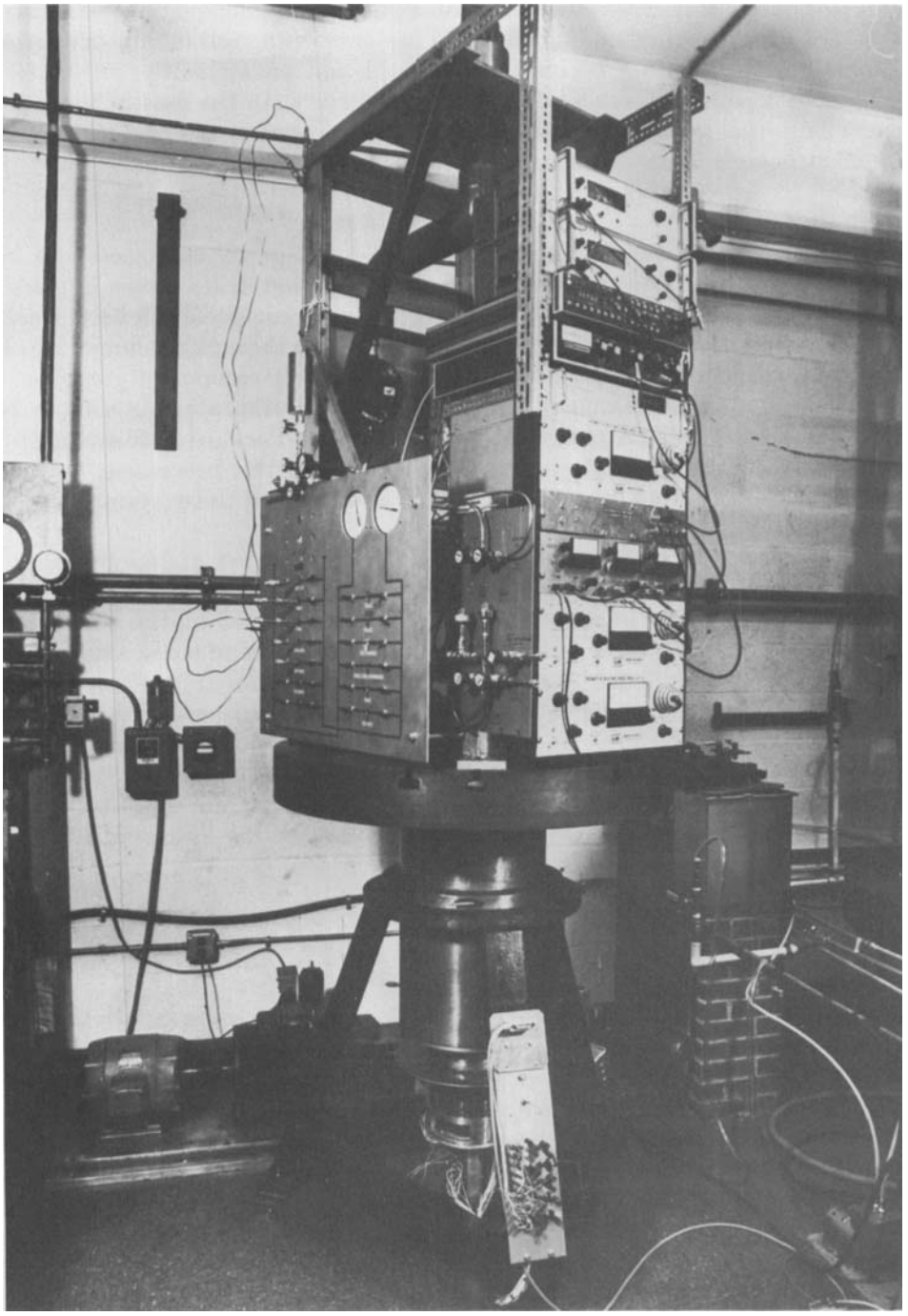

FIGURE 2. Photo of cryogenic Bénard apparatus on the 1 metre rotating table. The Graham drive is on the floor at the left, gas-handling panel is on the table, and the thermometry and temperature control is on the table to the right. Slip rings are on the bottom, and the bus cable is on the top of the patch panel.

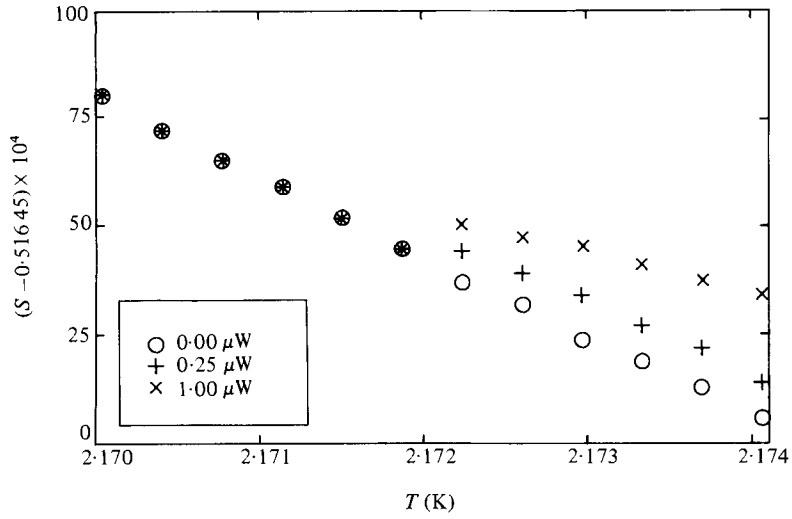

FIGURE 3. Test for parasitic heat input. Resistance ratio S plotted against temperature with different applied heat inputs H_F.

when data was taken out to the temperatures at which we ran our Bénard measurements.

4.2. *Thermometer calibration*

Calibration of the ratio S against the temperature difference ΔT with the C-boundary at a set temperature is achieved by varying the heat W_F into the F-boundary and measuring the values of R_F and S with fixed R_C. Calibrations at different values of T_C are obtained by repeating this procedure for different R_C settings. These measurements are made with the cell empty except for a very low density of ^{4}He gas. Using the zero-density values for thermal conductivity of ^{4}He gas (Ahlers 1978) we are able to obtain a measurement of the thermal resistance of the cell walls at the same time. The corresponding thermal conductivity of the stainless-steel walls agreed with published values within the uncertainty of those published values (see for example *Thermal Physical Properties of Matter*, 1970).

A separate calibration of the resistance thermometers R_F and R_C is required to complete the previous calibration. This is achieved by filling the cell with liquid ^{4}He and ensuring that there is zero power from H_F so that R_F and R_C are in thermal equilibrium. The C-regulator is used as before to adjust the cell temperature, and readings of R_C and R_F are taken against the pressure of the gas in the vapour-pressure bulb.

All these calibrations are made with the vacuum can evacuated to eliminate heat leaks to the bath other than through the copper braid. Once calibrations are made the cell is kept at helium temperatures for up to two months while Bénard measurements are made. However, even after a warm-up to room temperature and subsequent cool-down and recalibration we found the absolute calibration of R_F and R_C to be reproducible to 10^{-3} K and $dS/d\Delta T$ to 1 %.

5. Determination of the critical Rayleigh number

5.1. *Nusselt-number and Rayleigh-number calculations*

The Nusselt number is defined as the ratio of the measured thermal conductivity λ_m of a fluid at some temperature (in whatever state the fluid exists) to the thermal

Temperature (K)	ν (cm^2/s)	D_T (cm^2/s)	β_p (K^{-1})	λ (W/cm^2 K)
2·186	$1{\cdot}76\times10^{-4}$	$2{\cdot}32\times10^{-4}$	$5{\cdot}10\times10^{-3}$	$1{\cdot}65\times10^{-4}$
2·4	$2{\cdot}14\times10^{-4}$	$4{\cdot}19\times10^{-4}$	$3{\cdot}27\times10^{-2}$	$1{\cdot}46\times10^{-4}$
2·63	$2{\cdot}34\times10^{-4}$	$4{\cdot}76\times10^{-4}$	$4{\cdot}51\times10^{-2}$	$1{\cdot}57\times10^{-4}$
2·9	$2{\cdot}48\times10^{-4}$	$4{\cdot}89\times10^{-4}$	$5{\cdot}85\times10^{-2}$	$1{\cdot}70\times10^{-4}$
3·1	$2{\cdot}55\times10^{-4}$	$4{\cdot}78\times10^{-4}$	$6{\cdot}88\times10^{-2}$	$1{\cdot}78\times10^{-4}$
3·178	$2{\cdot}57\times10^{-4}$	$4{\cdot}71\times10^{-4}$	$7{\cdot}30\times10^{-2}$	$1{\cdot}80\times10^{-4}$
3·4	$2{\cdot}61\times10^{-4}$	$4{\cdot}44\times10^{-4}$	$8{\cdot}58\times10^{-2}$	$1{\cdot}87\times10^{-4}$
3·63	$2{\cdot}63\times10^{-4}$	$4{\cdot}17\times10^{-4}$	0·101	$1{\cdot}93\times10^{-4}$

TABLE 1. Sample of HeI parameters at indicated temperatures taken from the cubic-spline fits of Barenghi *et al.* (1981)

conductivity λ of that fluid at rest at the same temperature. Because in our experiment a finite amount of the heat dissipated by H_F conducts through the stainless-steel sidewalls, rather than through the helium, a correction to the measured conductance $W_F/\Delta T$ must be made in order to obtain a value for the measured thermal conductivity of the liquid helium. The thermal conductance of the helium is given by subtracting the conductance of the wall from the total conductance of the cell. The conductance of the wall is of course $1/R_w$, where R_w is its thermal resistance (mentioned in §4.2). The measured thermal conductivity for our cell is given by

$$\lambda_m = \frac{d}{A}\left(\frac{W_F}{\Delta T} - \frac{1}{R_w}\right),$$

where A is the cross-sectional area of the fluid, and ΔT is the measured temperature difference across the cell when W_F is the applied heat current. The thermal conductivity of the fluid at rest is obtained from the splined values given by Barenghi, Lucas & Donnelly (1981).

The Rayleigh number, defined in §2, is obtained from ΔT as measured and the appropriate fluid-parameter values also given by Barenghi *et al.* (1981). During an experiment both Nusselt numbers and Rayleigh numbers were evaluated at midplane temperatures to minimize effects of departures from the Boussinesq approximation (see Ahlers 1980). Table 1 lists a sample of the fluid parameters used.

5.2. *Experimental procedure and results*

An experiment began by filling the cryostat with liquid helium and stabilizing the bath and cell at the desired temperatures with W_F set to zero. The cryostat was set rotating when necessary and a period of time was provided (usually about 15 min) to ensure that thermal equilibrium was established as indicated by stability of all temperatures within a few μK. A set of measurements then consisted of stepping W_F through a range of values and measuring the ratio S. These values could then be converted to any desired form, such as ΔT versus W_F or Nu versus Ra as described in §5.1.

The experimental protocol for these measurements was the subject of a detailed investigation. Our preliminary data, reported in Lucas *et al.* (1981), were taken by advancing W_F in a continuous set of small steps and determining S by the automatic bridge, yielding a plot of S versus W_F. A clear break in this curve allowed a simple determination of R_c. The rate of advance of W_F was decreased until it was clear that R_c was independent of ramping rate.

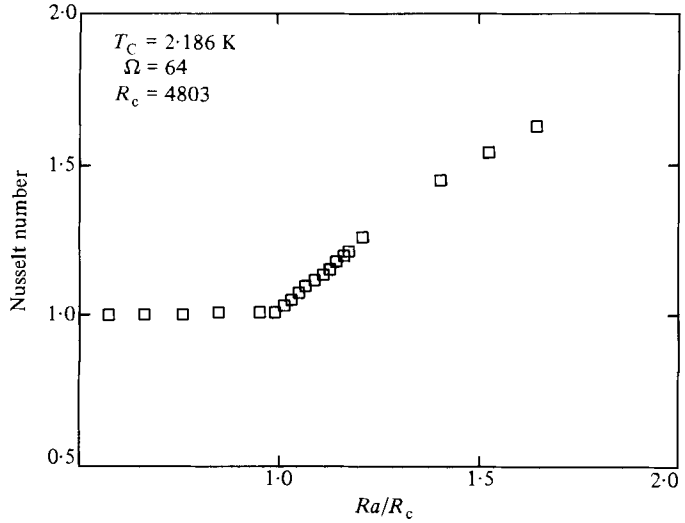

FIGURE 4. Heat transfer plot at $\Omega = 64$, $T_C = 2{\cdot}186$ K. Dependence of Nusselt number on Rayleigh number. The Rayleigh number is scaled by R_C.

Another way to determine R_c was reported by Ahlers & Behringer (1977). Here W_F is suddenly switched on from zero, and the response of the temperature of the floating side of the cell is recorded as a function of time. The details of the transient response yield a clear indication of the approach to equilibrium from above R_c, and a measure of the equilibration time. We determined the approximate value of R_c and the necessary waiting times for equilibration from such transient studies.

Our final protocol consisted of adjusting W_F to a given value, waiting for a predetermined time, taking a reading of S and adjusting W_F again. For values of $W_F < 0{\cdot}9W_{FC}$ (W_{FC} being the power producing a Rayleigh number of R_c) and for $W_F > W_{F(1{\cdot}2)}$ ($W_{F(1{\cdot}2)}$ being the power at which the resultant Nusselt number equalled 1·2) the waiting time was taken to be $t = 5\tau_D$, where $\tau_D = d^2/D_T$ is the thermal diffusion time. Typically τ_D is of the order of 1·5–3·0 min. For data in the critical region $0{\cdot}9W_{FC} < W_F < W_{F(1{\cdot}2)}$ the waiting time was set for $\frac{1}{2}$ h, or $10\tau_D$–$20\tau_D$.

Data taken in the above manner were reduced and displayed in the familiar Nu versus Ra form (cf. figure 4). To determine the critical Rayleigh number R_c we fitted a horizontal line to the points before the transition, and a quadratic to the points beyond. The intersection of these two curves was taken to define R_c, and it was determined that this procedure was in satisfactory agreement with the transient method and the S versus W_F method. Finally our data were plotted in the form Nusselt number versus Ra/R_c as shown in figure 4.

Data were taken at various temperatures indicated in table 2 with Prandtl values distributed throughout the possible range of HeI at the saturated vapour pressure. At 2·186 K we limited the data to the range of angular velocities $0 \leqslant \Omega \leqslant 64$ to avoid the critical temperature difference ΔT becoming comparable to $T - T_\lambda = 14$ mK, in which case the helium sample would have been seriously non-Boussinesq.

A summary of all the R_c data is shown in figure 5 and also in table 2.

5.3. *Uncertainties*

Our measurements of W_F and ΔT had maximum uncertainties of 0·5% and 5% respectively. The uncertainty in W_F was due to the least counts of the current and voltmeters, while the uncertainty in ΔT was due to the greater of two contributing

T_C (K)	Pr	Ω_D (rad/s)	Ω ($\Omega_D d^2/\nu$)	R_c
2·186	0·76	0	0	1262
		0·111	16	1595
		0·294	32	2536
		0·588	64	4803
2·4	0·51	0	0	1538
		0·269	32	2970
		0·539	64	5565
		0·809	96	8568
		1·079	128	11895
		1·350	160	15672
		1·621	192	19554
2·63	0·49	0	0	1444
		0·294	32	2937
		0·587	64	5510
		0·881	96	8616
		1·176	128	11878
		1·469	160	15513
		1·765	192	19370
2·9	0·51	0	0	1370
3·1	0·53	0	0	1489
3·178	0·55	0	0	1574
		0·323	32	3206
		0·646	64	5989
		0·969	96	9574
		1·292	128	13296
		1·615	160	17581
		1·938	192	21813
3·2	0·55	0	0	1473
3·4	0·59	0	0	1146
		0·328	32	2429
		0·657	64	5455
		0·985	96	8016
		1·313	128	11084
		1·641	160	14507
		1·970	192	18384
3·6	0·63	0·330	32	2501
		0·660	64	4715
		0·991	96	7386
		1·321	128	10607
		1·651	160	13483
		1·981	192	16716

TABLE 2. Summary of R_c dependence on dimensionless angular velocity

factors. Those factors affecting δT, the uncertainty in ΔT, were: (i) The resolution of the Texas Instruments pressure gauge, giving δT through a dP/dT relationship, and (ii) the variance in S with time, given δT through the calibration of S versus ΔT. The maximum 5 % uncertainty in ΔT corresponded to the high T_C, $\Omega = 0$ runs, and was less for lower T_C, $\Omega > 0$ runs. The uncertainties in the fluid parameters for HeI were obtained from the original sources quoted in Barenghi *et al.* (1981) and are listed in table 3. These uncertainties, combined with the maximum 5 % uncertainty in ΔT, the 0·5 % uncertainty in d and a maximum 0·1 % uncertainty in g gave a resultant 16 % maximum expected uncertainty in the Rayleigh number. This was calculated

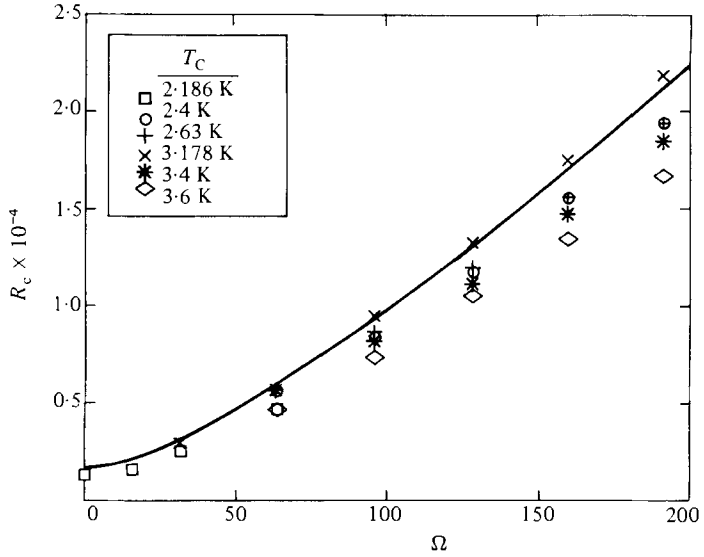

FIGURE 5. Rotational effects on R_c. Dependence of R_c on dimensionless angular velocity $\Omega = \Omega_D d^2/\nu$ and Prandtl number Pr. For clarity, not all data for $\Omega < 64$ is shown. The solid line represents the results of linear stability calculations. The scatter is considered to be due to errors in the determination of the thermodynamic and transport properties of HeI.

Parameter	Uncertainty (%)†	Parameter	Uncertainty (%)
T	±1	η	±5§
dP/dT	±0·06	β_D	±0·7
λ	±2‡	ρ	±0·4
C_S	±1		

† Listed here are the maximum values over the temperature range $2{\cdot}172\ \mathrm{K} < T < 4{\cdot}0\ \mathrm{K}$.
‡ The uncertainty was given through private communication with Prof. G. Ahlers.
§ The uncertainty was given through private communication with Prof. J. Goodwin.

TABLE 3. Uncertainties in fluid parameters of HeI used in calculation of Rayleigh numbers (obtained from original sources referenced in Barenghi *et al.* 1981)

in the manner in which one calculates the uncertainty Δ_X for a function $X = U^\alpha V/W$ given that $dU = \Delta_U U$, $dV = \Delta_V V$, and $dW = \Delta_W W$. (That is, the Δs times 100 give the percentage uncertainties in the respective parameters.) In particular, one finds $dX = (|\alpha\Delta_U| + |\Delta_V| + |\Delta_W|)U^\alpha V/W = (\Delta_X)X$. The maximum expected uncertainty in the Nusselt number was calculated in a similar fashion and was found to be 7 %. In practice the observed scatter in the Nusselt numbers before convection reached this value only for $\Omega = 0$ runs and was less than 2 % for all other runs.

6. Discussion

Figure 5 compares our experimental data with that predicted by linear theory. As can be seen from table 2 and figure 5 there are differences between our experimental determination of R_c and linear theory which vary irregularly with temperature. Most, but not all, of these differences fall within the expected 16 % uncertainty. Since

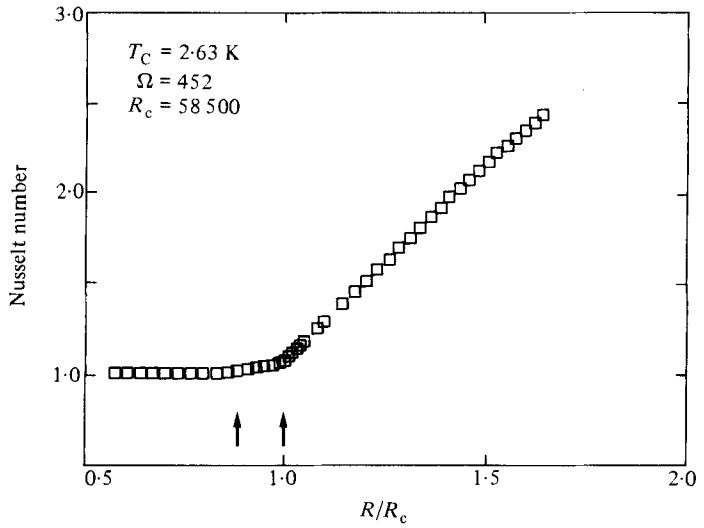

FIGURE 6. Subcritical convection. Dependence of Nusselt number on Rayleigh number. The first break in the data occurs at Rayleigh number less than that expected of linear convection. R_c, or the second break, occurs within expected uncertainty of value predicted by linear theory.

systematic errors in our procedures would vary smoothly with temperature, we conclude that the wide variation in R_c is due to faults in the thermodynamic and transport data. Additional points at $\Omega = 0$ alone (at 2·9, 3·1 and 3·2 K) have been taken to investigate in more detail temperature dependent variations in fluid-parameter uncertainties. In this paper we have resisted presenting our R_c ($\Omega > 0$) data normalized as was done in an earlier report (Lucas *et al.* 1981). The agreement between theoretical predictions for the dependence of R_c on Ω and our non-normalized data was the primary motivation for this change.

Our most recent experimental runs have demonstrated a characteristic of heat transfer in rotation uncommon to runs for which $\Omega < 200$. At higher rotation rates and using Nusselt-number–Rayleigh-number presentation of data we noticed two distinct breaks in our data (see figure 6). The first break was below the expected R_c and showed a small increase in Nusselt number. The second break occurred at the expected R_c (within the uncertainty expected) and displayed the more dramatic increase in Nusselt number common to steady convection. It is not presently clear what is responsible for this effect, but a consideration of centrifugal effects has proven to be illuminating. Both Koschmieder (1967) and Rossby (1969) have discussed the possibility that centrifugal forces are not negligible in their own experiments. Rossby has also shown heat-transfer effects due to subcritical convection in water at high Taylor number which look very similar to our own. It is perhaps interesting to note that, for similar-aspect-ratio cells, the ratio $\Omega_D^2 D/2g$ of the centrifugal to gravitational pressure-gradient terms in the equation of motion is greater than 0·002 for all cases in which this subcritical convection occurs in both Rossby's and our own experiments. This phenomenon is being further investigated and will be reported on in a future paper.

7. Conclusions

This experimental study demonstrates that there is agreement between experiment and linear stability theory over the angular-velocity dependence of the critical

Rayleigh number for the onset of convection in the cryogenic fluid ^{4}He in the hitherto unexplored range of Prandtl numbers $0{\cdot}49 < Pr < 0{\cdot}76$. Observations that the onset states are stationary over this range of Prandtl numbers for $\Omega < 200$ are consistent with the calculations of Clever & Busse (1979). It appears that there are substantial discrepancies in the measured thermodynamic and transport properties of HeI. Finally, for rotation rates $\Omega > 200$, or equivalently for $\Omega_D^2 D/2g > 0{\cdot}002$, a 'subcritical' convective mode is observed.

We are grateful for a number of useful discussions with Professors Guenter Ahlers, Friedrich Busse, Robert Behringer and Kwangjai Park. We acknowledge financial assistance from the National Science Foundation (U.S.A.) Heat Transfer Program grant CME 80-07478 and the Science and Engineering Research Council (U.K.). One of us (P.L.) is particularly grateful for the hospitality and facilities extended to him during two periods spent at the Department of Physics of the University of Oregon.

REFERENCES

AHLERS, G. 1974 Low temperature studies of the Rayleigh–Bénard instability and turbulence. *Phys. Rev. Lett.* **33**, 1185–1188.

AHLERS, G. 1975 The Rayleigh–Bénard instability at helium temperatures. In *Fluctuations, Instabilities and Phase Transitions* (ed. T. Riste), pp. 181–193. Plenum.

AHLERS, G. 1978 Thermal conductivity of ^{4}He vapor as a function of density. *J. Low Temp. Phys.* **31**, 429–439.

AHLERS, G. 1980 Effect of departures from the Oberbeck–Boussinesq approximation on the heat transport of horizontal convecting fluid layers. *J. Fluid Mech.* **98**, 137.

BARENGHI, C. F., LUCAS, P. & DONNELLY, R. J. 1981 Cubic spline fits to thermodynamic and transport properties of liquid ^{4}He above the λ-transition. *J. Low Temp. Phys.* **44**, 491–530.

BEHRINGER, R. P. & AHLERS, G. 1982 Heat transport and temporal evolution of fluid flow near the Rayleigh–Bénard instability in cylindrical containers. *J. Fluid Mech.* **125**, 219–258.

BUSSE, F. H. 1981 Transition to turbulence in thermal convection with and without rotation. In *Transition and Turbulence* (ed. R. E. Meyer), pp. 43–61. Academic.

CHANDRASEKHAR, S. 1953 The instability of a layer of fluid heated below and subject to Coriolis forces. *Proc. R. Soc. Lond.* **A 217**, 306–327.

CHANDRASEKHAR, S. 1961 *Hydrodynamic and Hydromagnetic Stability.* Clarendon.

CHARLSON, G. S. & SANI, R. L. 1970 Thermoconvective instability in a bounded cylindrical fluid layer. *Int. J. Heat Mass Transfer* **13**, 1479–1496.

CLEVER, R. M. & BUSSE, F. H. 1979 Nonlinear properties of convection rolls in a horizontal layer rotating about a vertical axis. *J. Fluid Mech.* **94**, 609–627.

DANIELS, P. G. 1978 Finite amplitude two-dimensional convection in a finite rotating system. *Proc. R. Soc. Lond.* **A 363**, 195–215.

DROPKIN, D. & GLOBE, S. 1959 Effect of spin on natural convection in mercury heated from below. *J. Appl. Phys.* **30**, 84–89.

FULTZ, D. & NAKAGAWA, Y. 1955 Experiments on over-stable thermal convection in mercury. *Proc. R. Soc. Lond.* **A 231**, 211–225.

GOROFF, I. 1960 An experiment on heat transfer by overstable and ordinary convection. *Proc. R. Soc. Lond.* **A 254**, 537–541.

KOSCHMIEDER, E. L. 1967 On convection on a uniformly heated rotating plane. *Beit. zur Phys. der Atmos.* **40**, 216–225.

KRISHNAMURTI, R. 1971 On the transition to turbulent convection. In *Proc. 8th Symp. on Naval Hydrodynamics, Rep. ARC-179*, 289–310, *Office of Naval Research.*

KÜPPERS, G. 1970 The stability of steady finite amplitude convection in a rotating fluid layer. *Phys. Lett.* **A 32**, 7–8.

KÜPPERS, G. & LORTZ, D. 1969 Transition from laminar convection to thermal turbulence in a rotating fluid layer. *J. Fluid Mech.* **35**, 609–620.

LEE, G., LUCAS, P. & TYLER, A. 1979 Bénard instability measurements in ^{3}He–^{4}He mixtures near their lambda temperatures. *Phys. Lett.* **75A**, 81–84.

LUCAS, P. & DONNELLY, J. A. 1981 Computer-automated ratio transformer bridge. *Rev. Sci. Instrum.* **52**, 582–584.

LUCAS, P., PFOTENHAUER, J. M. & DONNELLY, R. J. 1981 Rotating cryogenic Bénard cell. (In *Proc. 16th Int. Conf. on Low Temp. Phys.* LT16) *Physica* **107B**, 147–148.

MAURER, J. & LIBCHABER, A. 1980 Effect of the Prandtl number on the onset of turbulence in liquid ^{4}He. *J. Physique Lett.* **41**, 515.

NAKAGAWA, Y. & FRENZEN, P. 1955 A theoretical and experimental study of cellular convection in rotating fluids. *Tellus* **7**, 1–21.

ROSSBY, H. T. 1969 A study of Bénard convection with and without rotation. *J. Fluid Mech.* **36**, 309–335.

Thermal Physical Properties of Matter, TPRC Data Series, vol. 1, 1970, pp. 1164–1175. Plenum.

VERONIS, G. 1968 Large-amplitude Bénard convection in a rotating fluid. *J. Fluid Mech.* **31**, 113–139.

WALDEN, R. W. & AHLERS, G. 1981 Non-Boussinesq and penetrative convection in a cylindrical cell. *J. Fluid Mech.* **109**, 89–114.

WARKENTIN, P. A., HAUCKE, H. J., LUCAS, P. & WHEATLEY, J. C. 1980 Stationary convection in dilute solutions of ^{3}He in superfluid ^{4}He. *Proc. Natl Acad. Sci.* **77**, 6983–6987.

WHITE, G. K. 1979 *Experimental Techniques in Low-Temperature Physics.* Clarendon.